

The reference altitude upon which μ , ρ , and α' are to be selected is clearly arbitrary.

IV. Conclusions

For a specific type of craft which is structurally and geometrically similar, a plot may be established for the coefficients $\bar{\alpha}_i'$ and $\bar{\beta}_i'$ against relative mass μ . For engineering approximations of the wing natural frequencies, it is only necessary to compute μ , interpolate values of the coefficients $\bar{\alpha}_i'$ and $\bar{\beta}_i'$, and specify the semispan length. This method of approximation is feasible for all types of craft as long as similarity characteristics within each class is preserved.

References

- ¹Hillard, S. E. and Sevik, M. M. "Determination of Critical Nondimensional Parameters in Aircraft Dynamic Response to Random Input," CR-2361, Jan. 1974, NASA.

Cambered Joukowski Airfoil in a Nonuniform Weak Shear Flow

A. K. Gupta* and S. C. Sharma†

Indian Institute of Technology, Kanpur, India

THE analysis by Tsien,¹ Sowryda,² and Jones³ of symmetrical and cambered Joukowski airfoils placed in two-dimensional uniform and nonuniform shear flows have predicted an increase in lift and pitching moment characteristics compared to the values of uniform flow. The results for symmetrical Joukowski airfoils have been tested experimentally by Vidal⁴; Vidal, Hilton, and Curtis⁵; and Ludwig and Erickson Jr.⁶ for the values of shear parameter equal to about two to five. Furthermore, their experiments carried out in a two dimensional nonuniform shear flow simulating a propeller slipstream showed that the airfoil characteristics depended upon the location of the airfoil and the product of local stream shear with the shear derivative.

An experimental investigation was undertaken to extend the measurements to the cambered Joukowski airfoil placed in a two-dimensional nonuniform weak shear flow. The results of this investigation are presented in this Note.

Experiments

A 6 in. chord, 12 in. span Joukowski airfoil of thickness ratio τ of 0.15 and camber of 0.10 was made out of seasoned wood. The coordinates of the Joukowski profile were obtained by the method given in Ref. 7. Twenty-three static pressure holes of diameter 0.032 in. were made along the midspan chord, and an equal number of pressure leads were taken out of a $\frac{3}{4}$ in. o.d. tube fitted in the center of the left tip of the airfoil. The axis of the $\frac{3}{4}$ in. tube coincided with the midchord axis, and the airfoil was pitched about this axis. To obtain the nonuniform weak shear flow, a screen using horizontal aluminum rods of $\frac{1}{4}$ in. and $\frac{1}{2}$ in. diam was built following the steps out-

Fig. 1a Screen; flow from left to right.

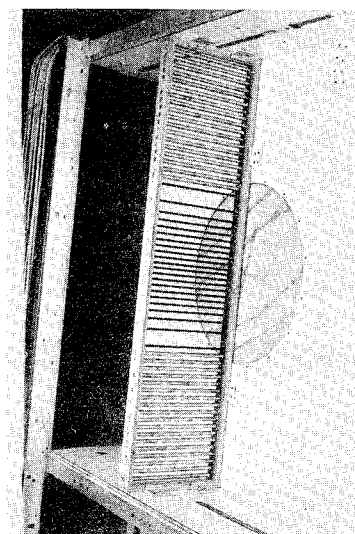


Fig. 1b Airfoil.

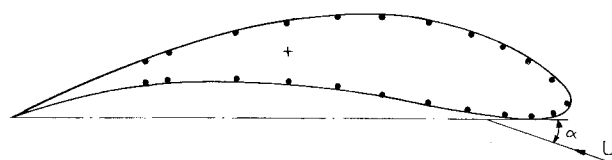
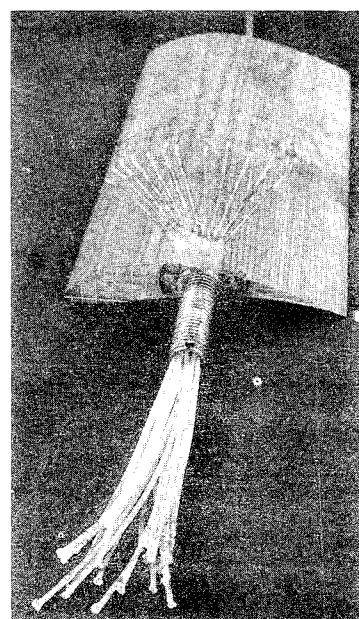


Fig. 1c Cambered Joukowski airfoil: chord 15 cms; thickness 15%; camber 10%; static pressure taps (-).

lined in Ref. 5 and 6. Pictures of the screen mounted in the wind-tunnel test section, of the cambered Joukowski airfoil, and a sketch of the contour of the airfoil chord with static pressure locations marked by dots are shown in Figs. 1a-c, respectively.

The experiments were carried out in a closed-circuit, closed-jet, low-speed wind tunnel at IIT Kanpur. The test section of the wind tunnel is 4 ft high, 1 ft wide, and 5.5 ft long. It has a contraction ratio of 9.5 and a turbulence level of 1.4% at the maximum wind speed of 180 fps. Two fans mounted one on top of the other in the return circuit are driven by two motors of 15 hp each. A velocity traverse in the vertical direction made in the clear test section showed a $\pm 1.5\%$ variation in mean velocity across the test section height.

The two-dimensional airfoil which spanned the 1 ft width of the test section was located 36 in. downstream of

Received February 13, 1974, revision received May 22, 1974.
Index categories: VTOL Aircraft Design; Jets, Wakes, and Viscid-Inviscid Flow Interactions.

*Assistant Professor, Department of Aeronautical Engineering.

†Present Address: Aerodynamics Division, Vikram Sarabhai Space Centre, Trivandrum, Kerala, India.

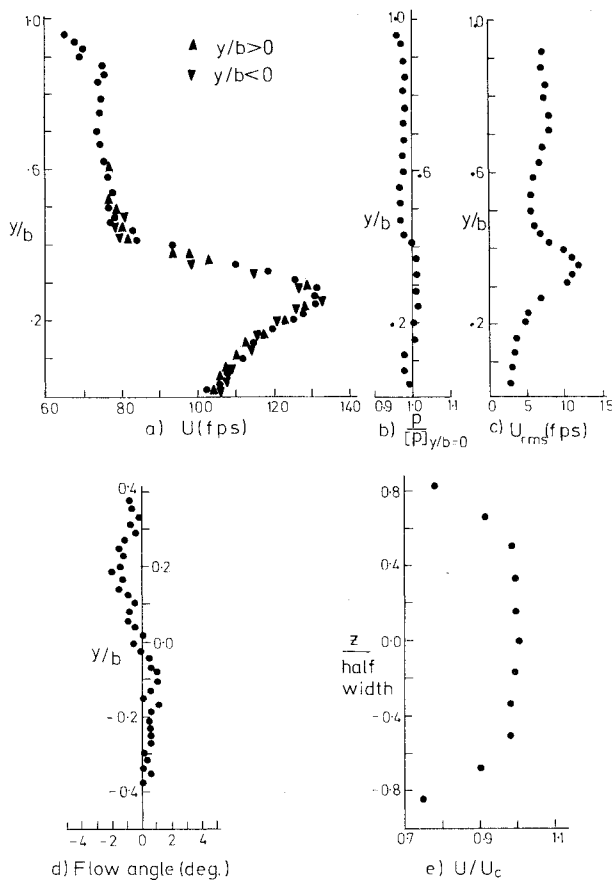


Fig. 2 Nonuniform shear flow characteristics: $b = 24$ in. = test section half height.

the screen⁶ with a provision to move it up or down in the vertical plane at several discrete locations. A sharp edge pointer was fixed to the $\frac{3}{4}$ in. diam tube of the airfoil, and the pitch angles were read on a 360° protractor with a resolution of $\frac{1}{2}^\circ$. Static pressures were read on an inclined (30° with the vertical), 100 tubes, water multitube manometer with a resolution of 1 mm in height.

The mean velocity profile at the airfoil location vertical plane was measured with two types of probes. In one case, a $\frac{3}{8}$ in. diam pitot-static tube was traversed in the upper half of the test section in steps of 1 in. Secondly, a vertical pitot comb with 40 tubes, each of $\frac{1}{16}$ in. diam, spaced $\frac{3}{4}$ in. apart spanning the central 30 in. height of the test section was employed to measure the local stagnation pressures. The static pressure was measured by 4 evenly spaced tubes out of 40 in the pitot comb.

The two dimensionality of the mean flow was measured with another horizontal pitot rake, which had 11 pitot tubes of $\frac{1}{16}$ in. diam, spaced 1 in. apart. Two tubes out of eleven located symmetrically 3 in. off center were pitot-static tubes.

The flow angle was measured by means of a cylindrical probe of $\frac{1}{8}$ in. diam, and 12 in. in length, the axis of which was perpendicular and horizontal to the mean flow direction. Two pressure holes of 0.02 in. diam were made 72° apart on the circular periphery in a plane about $\frac{1}{2}$ in. from one sealed tip of the cylindrical probe, and the two leads from these pressure holes were taken out of the other tip to connect to a water multitube manometer. The other tip of the $\frac{1}{8}$ in. diam probe was keyed to a 4 in. diam disk marked on its periphery with protractor-like graduations with a resolution of one degree. A pointer indicated the amount of rotation in degrees of the cylindrical probe about its axis. The flow angle probe assembly was mounted on a tripod stand fitted with a rack and pin-

ion-type vertical traverse arrangement. The cylindrical probe was inserted into the test section at the airfoil location vertical plane through a side panel which had $\frac{1}{8}$ in. diam holes spaced $\frac{1}{2}$ in. apart interval vertically. The flow angle was measured by rotating the cylindrical probe about its axis until the same pressure from the 72° apart two pressure holes was observed on the manometer.

A 0.0005 in. diam, $\frac{1}{8}$ in. long Wollaston Platinum single hot wire probe along with a DISA, Model 55 A01, constant temperature anemometer was used to measure the turbulence level.

Results

The mean flow characteristics at a station approximately 36 in. downstream of the screen are shown in Figs. 2a-e. Two sets of mean velocity data, one obtained with the pitot-static tube and the other with the pitot comb are plotted in Fig. 2a. Data points in the lower half of the test section are also plotted in the upper half plane. It is seen that the mean velocity data from two independent probes collapse on a single profile, indicating thereby its reliability. Furthermore, in the range $-0.6 < y/b < 0.6$, where the data were available from the pitot comb, the symmetry of mean flow about $y/b = 0$ is well established. 'b' denotes the half height of the test section and is equal to 24 in.

The static pressure distribution and the rms streamwise fluctuating velocity are shown in Figs. 2b, and c, respectively. The static pressure distribution was measured with the pitot static tube and has been normalized with the static pressure measured at $(y/b) = 0$. For $(y/b) \leq 0.1$ (or $(y/r) \leq 0.33$, where 'r' is the distance in y direction measured from $(y/b) = 0$ at which the mean velocity is a maximum), the static pressure variation is within 2%, and the turbulence level is approximately constant at 3%.

The data on flow angle obtained with the $\frac{1}{8}$ in. diam cylindrical null type probe described earlier are plotted in Fig. 2d. A positive angle implies an upward flow inclination. A null-type flow angle measuring probe like the one used in the present investigation will indicate an apparent flow inclination. This apparent flow inclination will be negative in a positive shear and positive in a negative shear. This is precisely the trend shown by data in Fig. 2d, where flow inclinations are negative for $(y/b) > 0$, and are positive for $(y/b) < 0$.

The mean velocity profile in the spanwise direction at $y/b = 0$, 36 in. downstream of the screen is shown in Fig. 2e. Boundary layers on the side walls are about 3 in. thick and are most probably turbulent. The central 6 in. core of the flow has a uniform velocity within 2%.

From the measured pressure distributions over airfoils, pressure coefficients, $C(p_u)$ and $C(p_l)$, based on midchord dynamic pressure were computed on the upper and lower surfaces. Section lift coefficients, C_L , were computed using the following relations:⁷

$$C_n = - \int_0^1 (C_{p_u} - C_{p_l}) d\left(\frac{x}{c}\right)$$

$$C_c = \oint C_p d\left(\frac{y}{c}\right)$$

$$C_L = C_n \cos \alpha - C_c \sin \alpha$$

where C_n , C_c , α , and c are force coefficients normal and parallel to the chord axis, angle of attack, and chord, respectively. Since the values of pressure coefficients were known at discrete locations on the airfoil, a numerical integration using the 'Trapezoidal area rule' was carried out on an IBM 7044 computer.

The trailing-edge quarter chord presented a problem in computation. Since the static pressure taps could not be located in this region due to its thinness, an estimate of

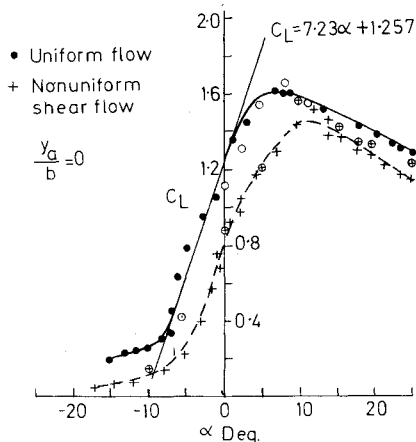


Fig. 3a Section lift coefficient of a cambered Joukowski airfoil. $\tau = 0.15$, $h/c = 0.10$.

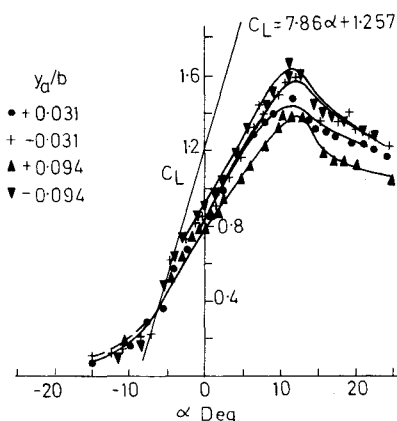


Fig. 3b Section lift coefficient of a cambered Joukowski airfoil at various vertical locations.

pressure coefficients in this region was made by assuming that $(C_p)_{\text{trailing edge}}$ was zero, and extrapolating the known pressure coefficients for $x/c \leq 0.75$ in the region $0.75 < x/c < 1$. Actually, $(C_p)_{\text{trailing edge}}$ depends on the angle of attack and is, in general, nonzero by a small amount. However, we believe that the error in C_L because of this assumption is likely to be small,⁸ leaving the inferences drawn from C_L vs α plots unaltered.

The results so obtained are plotted in Fig. 3a as C_L vs α for the cambered Joukowski airfoil placed in uniform flow and in the nonuniform shear flow at $(y_a/b) = 0$. ' y_a ' denotes the ' y ' coordinate of the airfoil midchord center. The Reynolds number based on the airfoil chord is approximately 3×10^5 . Theoretical line $C_L = 7.23\alpha + 1.257$ for the uniform flow corresponding to 15% thickness ratio and 10% camber is also shown.

In uniform flow, the theoretical line and experimental data near $\alpha = 0$ are in good agreement. In the nonuniform weak shear flow, on the other hand, the data points show a loss in lift near $\alpha = 0$ with only a marginal improvement in stalling. Both of these tests were repeated after a period of six weeks, and the repeat data points are shown enclosed in circles. No correction in the mechanical angle of attack due to local flow inclination has been applied. The reason for this is discussed later.

Figure 3b shows C_L vs α curves for the cambered Joukowski airfoil at different locations $(y_a/b) = \pm 0.031$, ± 0.094 ($y_a/r = \pm 0.103$, ± 0.313) in the nonuniform weak shear flow. Again, midchord dynamic pressure has been used to form section lift coefficients. A dependence of the aerodynamic characteristics on the position of the airfoil is evident. In particular, the maximum lifts are greater for $(y_a/b) < 0$ compared with $(y_a/b) > 0$. A similar observation concerning the dependence of aerodynamic character-

istics on airfoil location has been made by Vidal⁴ and by Ludwig and Erickson Jr.⁶ for a symmetrical Joukowski airfoil placed in significantly stronger nonuniform shear flows. Near $\alpha = 0$, however, the lift of a cambered Joukowski airfoil at all locations in the present nonuniform weak shear flow is less than the lift in uniform flow.

Discussion

Near $(y/b) = 0$, the nonuniform shear mean velocity profile can be approximated by a form^{3,4}

$$U = U_c \left[1 + \frac{q}{2} \left(\frac{y}{H} \right)^2 \right]$$

where U_c is the velocity at $(y/b) = 0$, q is a shear parameter and H is a transformation length which is equal to 1.7 in. for the present airfoil. With $U_c = 103.5$ fps and $U = 123$ fps at $(y/b) = 0.2$, one finds q to be 0.0476. Thus $q \ll 1$, and Jones' analytical results should be applicable. The actual mean velocity profile near $(y/b) = 0$ in Fig. 2a agrees only approximately with the parabolic mean velocity profile

$$U = 103.5 \left[1 + \frac{0.0476}{2} \left(\frac{y}{1.7} \right)^2 \right]$$

For $q \ll 1$, Jones' analysis gives the following expression for the lift coefficient:

$$C_L = \frac{2L}{\rho U^2 c} \approx 2\pi\alpha[1 + \tau - q(0.8841 + \ln q)] + 4\pi \frac{h}{c}$$

With

$$q = 0.0476, \tau = 0.15, \text{ and } \frac{h}{c} = 0.10, \text{ we obtain}$$

$$C_L \approx 7.86\alpha + 1.257$$

This is also shown in Fig. 3b as a solid line. Apparently, according to both Jones' and Sowryda's analysis, there is no interaction between the stream shear and camber up to first order in q . And yet a decrease in lift characteristics near $(y/b) = 0$ is indicated by data in Figs. 3a and b.

At this point, the magnitude of apparent flow inclination given by the null-type flow angle measuring probe can also be estimated. Let us consider the $\frac{1}{8}$ in. diam cylindrical probe is located at $(y/b) = 0.1$ with the plane of the probe, about which the two pressure holes are symmetric, parallel, and horizontal to a parallel positive shear flow. For the present parabolic mean velocity profile with $q = 0.0476$, the wind speeds at the upper and lower hole locations differ by 0.75 fps approximately with the mean speed on the center plane of the probe equal to 108.4 fps. The velocity component normal to pressure hole is obtained by multiplying the parallel mean velocity at that hole by cosine of 36° . Thus small clockwise rotation of the cylindrical probe about its axis will provide null. This amount of clockwise rotation for positive shear has been estimated to be close to $\frac{3}{4}^\circ$. With this correction in the measured flow inclination in Fig. 2d, the variation of the mean flow inclination is less than about one degree, which is within the present experimental accuracy. Ludwig and Erickson Jr.⁶ have applied a local correction of less than 2° to their mechanical angle of attack. But, in view of the variation of their measured flow inclination from -1° to about $+2^\circ$ over a typical vertical distance equal to the thickness of their airfoil, it is not clear to us what significance can be attached to their correction.

To separate the effect of thickness alone, and to compare data with existing results,⁴⁻⁶ a symmetrical Joukowski airfoil of 6 in. chord and 15% thickness ratio was made and tested in the same uniform and nonuniform weak shear flows at $(y_a/b) = 0$. The data are presented in Fig. 4. Theoretical line for the uniform flow, Vidal's data

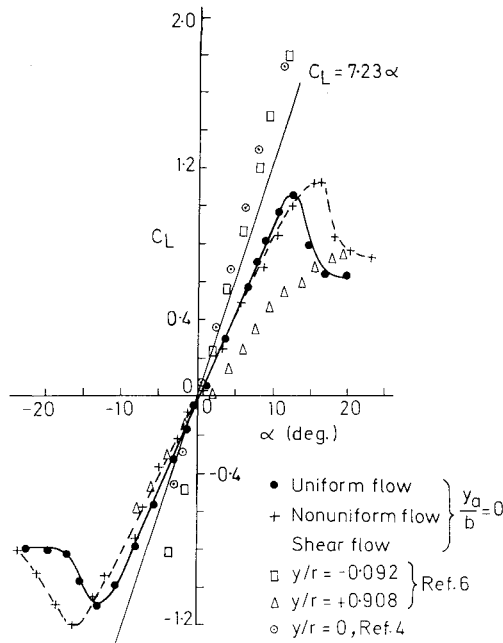


Fig. 4 Section lift coefficient of a symmetrical Joukowski airfoil $\tau = 0.15$.

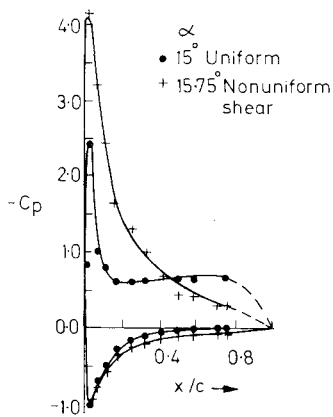


Fig. 5a Pressure coefficient on a symmetrical Joukowski airfoil.

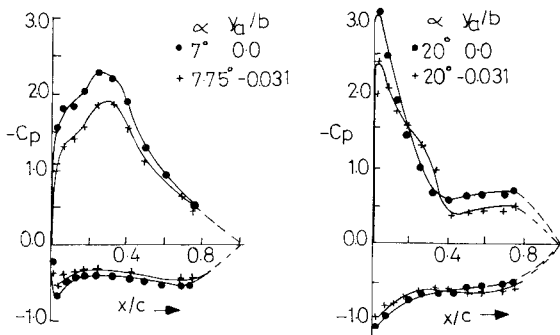


Fig. 5b Pressure Coefficient on a cambered Joukowski airfoil. Uniform flow; nonuniform shear flow (+).

points corresponding $(y_a/r) = 0$, and local shear parameter of about two, and Ludwig and Erickson Jr.'s data points⁶ corresponding to $(y_a/r) = -0.092$, $+0.908$, and a shear parameter of five are also included.

The investigations on symmetrical Joukowski airfoils have concluded that the measured pressure distributions

and therefore the lift coefficients near $\alpha = 0$ are in agreement with the computed values^{4,6} provided that the numerical computations take into account the presence of slipstream free streamlines and the tunnel boundaries. Thus, the inviscid interaction of stream shear with thickness is predictable for small angles of attack. Stalling, on the other hand, is a viscous flow phenomenon and occurs because of separation of the boundary layer on the upper surface of the airfoil. In the present context, one has to consider the behavior of a boundary layer in a freestream with shear and a streamwise pressure gradient. Vidal's analytical study⁴ has shown that boundary-layer shear interaction is negligible, and it is the inviscid interaction with shear producing a pressure distribution which is likely to control stalling characteristics. At present, no generalization about stalling characteristics and its dependence on airfoil vertical location can be made.

The data in Fig. 4 show a slight increase in maximum lift and destalling in the nonuniform weak shear flow. This is in reasonable agreement with the results of Refs. 4-6, where tests were conducted in significantly stronger shear flows. Thus, the loss of lift characteristics of a cambered Joukowski airfoil near $\alpha = 0$ as shown in Figs. 3a and b seems to be due to an interaction of camber with weak shear.

To get some insight into the reasons for loss of lift, some typical pressure distributions both for symmetrical and cambered Joukowski airfoils are shown in Figs. 5a-c. The pressure coefficients, C_p , are based on midchord dynamic pressures. They indicate that the changes in lift and stalling characteristics are due to the changes in pressure distribution over the upper surface of the airfoils. No noticeable variation of stagnation streamlines is discernible, perhaps because of the weak shear flow. The effect of free-stream turbulence is largely beneficial near stalling, and as noted by Vidal,⁴ the destalling is likely to be both due to shear and the increase in freestream turbulence.

The present experiments indicate that a cambered Joukowski airfoil when placed in a nonuniform weak shear flow shows a loss in lift characteristics near $\alpha = 0$, which is not predicted by uniform shear or simple nonuniform shear flow theories. Numerical computations for cambered Joukowski airfoils in nonuniform shear flows and further experiments in stronger shear flows will be helpful in explaining these observations.

References

- 1Tsien, H. S., "Symmetrical Joukowski Airfoils in Shear Flow," *Quarterly of Applied Mathematics*, Vol. 1, 1943, pp. 130-148.
- 2Sowryda, A., "Theory of Cambered Joukowski Airfoils in Shear Flow," Rept. AI-1190-A-2, Sept. 1958, Cornell Aeronautical Lab., Buffalo, N.Y.
- 3Jones, E. E., "The Forces on a Thin Airfoil in Slightly Parabolic Shear Flow," *Zeitschrift für Angewandte Mathematik und Mechanik*, Vol. 37, No. 9-10, 1957, pp. 362-370.
- 4Vidal, R. J., "The Influence of Two Dimensional Stream Shear on Airfoil Maximum Lift," *Journal of Aerospace Sciences*, Vol. 29, No. 8, 1962, pp. 889-904.
- 5Vidal, R. J., Hilton, J. H., and Curtis, J. T., "The Two Dimensional Effects of Slip-Stream Shear on Airfoil Characteristics," Rept. AI-1190-A-5, Sept. 1960, Cornell Aeronautical Lab., Buffalo, N.Y.
- 6Ludwig, G. R. and Erickson, J. C. Jr., "Airfoils in Two Dimensional Non-Uniformly Sheared Slip-Stream," *Journal of Aircraft*, Vol. 8, No. 11, Nov. 1971, pp. 874-884.
- 7Houghton, E. I. and Brock, A. E., *Aerodynamics for Engineering Students*, Edward Arnold Ltd., London, 1966.
- 8Schlichting, H., *Boundary Layer Theory*, 4th ed., 1962, McGraw-Hill, New York, Chap. I, p. 21.